DOI: 10.1002/cphc.201100663

Intrinsic Property of Flavin Mononucleotide Controls its Optical Spectra in Three Redox States

Yue-jie Ai,[a] Guangjun Tian,[a] Rong-zhen Liao,[c] Qiong Zhang,[a] Wei-hai Fang,*[b] and Yi Luo*[a, d]

Optical spectroscopic techniques have been the primary tools in detecting peptide conformation dynamics,[1] protein folding,[2] local solvation dynamics,[3] electron transfer processes,[4] and photochemical reactions.[5] The spectra reflect molecular properties in both internal (e.g. molecular structure and charge distribution) and external (environmental) aspects. In particular, the environmental influence can be classified into implicit and specific interactions between the system and the surrounding protein or solvents. These long-range and short-range interactions play an important role in biological molecules, also regulating their biological functions and activities. Revealing the connection of internal and external properties and their roles in the biological reactions has become the most challenging task for spectroscopic experimentalists because of the complexity and the dynamics of the external environment. There is an obvious gap between actual spectral information and possible interpretations, which could only be filled by theoretical modeling, which is capable of providing fine structures of spectral profiles, such as vibrational progressions.

Herein, we use flavin mononucleotide (FMN) as a model system to demonstrate the importance of theoretical modeling and its power to reveal details that cannot be accessed directly by measurements.

Flavodoxin as a flavoprotein is much involved in a variety of biochemical and physiological functions, such as interchangeability with ferredoxins, carbon dioxide and nitrogen fixation, oxygen activation, and so forth.[6] Its practical applications in the design of protein/metal nanostructures or drugs have drawn much attention recently.[6b] Flavodoxin contains FMN as a cofactor, which is non-covalently bonded to flavodoxin, expressing its redox activity through electron transport between different oxidation states. This intrinsic property was suggested to be tailored by the host apoprotein.[6a] Due to its important role in biological functions and its unique redox properties, FMN has been extensively studied by experimentalists and theoreticians.[6b] Recently, Chang et al. characterized the different ultrafast solvation dynamics of the three redox states (the oxidized form FMN, semiquinone $FMNH^{\bullet}$ and hydroquinone $FMNH^{-}$, Figure 1 a) by ultrafast femtosecond measurements,

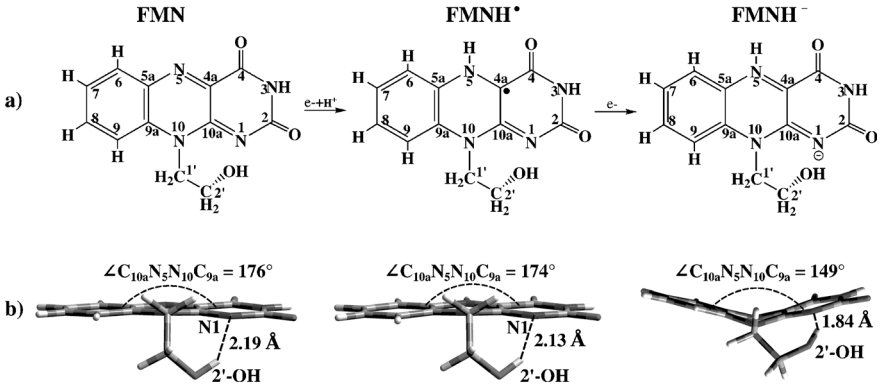

Figure 1. a) The three redox states of the FMN cofactor and their connections. b) Optimized structures of the three redox states.

which are suggested to arise from the local protein plasticity and water network flexibility.[3] We calculated vibrationally-resolved absorption spectra of the three redox states of FMN and obtained excellent agreement with the experimental spectra. However, our results indicate that specific short-range interactions play a negligible role in the determination of the optical spectra of FMN in its three different redox states, while the intrinsic properties play an important role.

The initial geometries were extracted from X-ray crystal structures of Desulfovibrio vulgaris flavodoxins in the three different redox states[7] (PDB codes:2FX3, 2FX4, 2FX5), with manually added hydrogens. The models with intramolecular hydrogen bonds, including the isoalloxazine ring, are shown in Figure 1 a. The ground-state structures were optimized using density functional theory with the hybrid functional B3LYP. The excitation energy and oscillator strength of the excited states were calculated with time-dependent density functional theory (TDDFT) based on the optimized geometries of the ground

[a] *Dr. Y.-j. Ai, G. Tian, Q. Zhang, Prof. Y. Luo*
Theoretical Chemistry and Biology, School of Biotechnology
Royal Institute of Technology
Roslagstullsbacken 15, 10691 Stockholm (Sweden)
Fax: (+46) 855378590
E-mail: luo@kth.se

[b] *Prof. Dr. W.-h. Fang*
College of Chemistry, Beijing Normal University
No.19, XinJieKouWai St., 100875 Beijing (P. R. China)
E-mail: fangwh@bnu.edu.cn

[c] *Dr. R.-z. Liao*
Department of Organic Chemistry, Stockholm University
10691 Stockholm (Sweden)

[d] *Prof. Y. Luo*
Heifei National Laboratory for Physical Science at the Microscale
University of Science and Technology of China
Heifei, 230026 Anhui (P. R. China)

states. A standard 6-311++G(2d,2p) basis set was used for all the calculations. The polarization effects of the enzyme environment were considered by the polarizable continuum model (PCM).[8] In the PCM model, the protein environment is represented by a homogeneous dielectric medium surrounding the reaction cavity. Herein a dielectric constant of 4 was typically chosen, as it has for modeling enzymes elsewhere.[9] The quantum mechanics/molecular mechanics (QM/MM) approach was used to explore the specific effects from the external protein environment by applying the ONIOM[10] (B3LYP:Amber) method. Starting from the protein crystallographic coordinates (PDB code 2FX5), the $FMNH^-$ molecule was treated as the quantum mechanical (QM) part and was optimized at the B3LYP level. The remaining protein environment was treated as the molecular mechanical (MM) part utilizing the Amber force field. The MM part was fixed at the crystal coordinates during the geometry optimizations. All the geometry optimizations and excited-state calculations were performed using the Gaussian 09 software package.[11] The vibrationally-resolved absorption spectra were calculated using the linear coupling model (LCM).[12] Herein, the contributions of the first ten excited states were included in the simulated spectra. The line-shape broadening of the computed spectra were described by Lorentzian functions with half width at half maximum (HWHM) is equal to 0.05 eV for vibrationally-resolved spectra and 0.1 eV for pure electronic spectra.

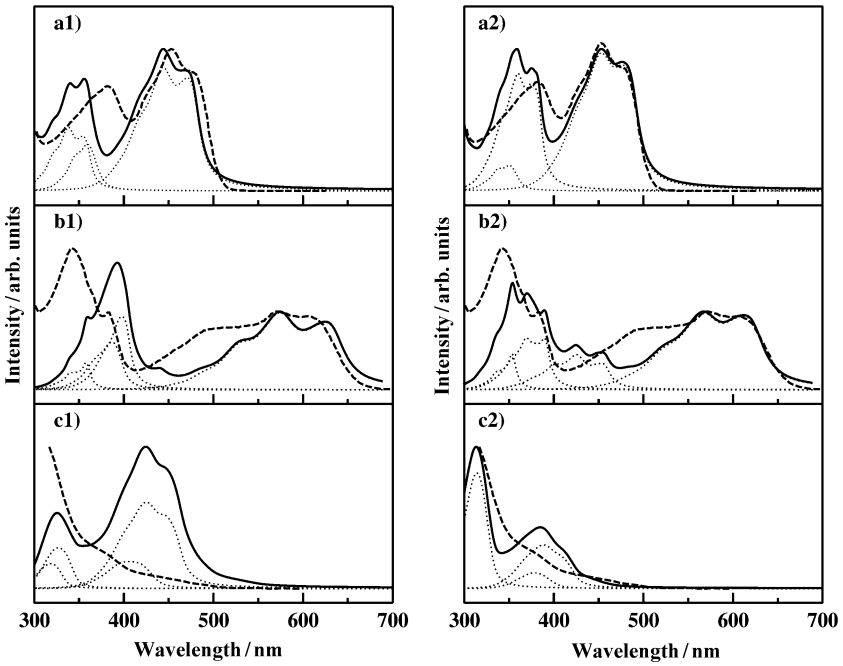

Figure 2. Calculated vibrationally-resolved absorption spectra for a) FMN, b) $FMNH^{\bullet}$, and c) $FMNH^-$ in the gas phase (left) and including PCM (right), indicated by the solid line in both cases. The corresponding experimental spectra (-----) are shown for comparison. The dotted lines represent the contributions of some individual excited states. The calculated spectra are shifted by −0.47, −0.20, and −0.47 eV for FMN, $FMNH^{\bullet}$, and $FMNH^-$, respectively. The experimental spectra are taken from ref. [3].

The redox center of the FMN molecule is the aromatic triple ring isoalloxazine. In an earlier study on the anionic hydroquinone ($FADH^-$), we found that the intramolecular hydrogen bonding between the linking ribityl chain and the isoalloxazine plays an important role in its photochemical properties.[13] As shown in Figure 1b, the intramolecular hydrogen bonds between N1 and 2′-OH are 2.19 Å, 2.13 Å and 1.84 Å for FMN, $FMNH^{\bullet}$, and $FMNH^-$, respectively. With the injection of two electrons, N1 becomes negatively charged and thus a stronger hydrogen bond is formed. Another distinct difference in the geometric structures of the three redox states is the planarity of the isoalloxazine ring. The neutral and radical species possess a relative planar isoalloxazine ring, with a dihedral angle $C_{10a}N_5N_{10}C_{9a}$ of 176° and 174°, respectively. The anionic $FMNH^-$ molecule has a butterfly bending angle of 149°. The folded butterfly conformation has been commonly found in reduced species of flavins.[14]

The calculated absorption spectra for the three redox states in gas-phase and the PCM model are shown in Figure 2. For better comparison they were calibrated with respect to the corresponding experimental spectra (-----). The uniform energy shifts for FMN, $FMNH^{\bullet}$ and $FMNH^-$ are −0.47, −0.20, and −0.47 eV, respectively. We also plotted the spectra for several individual excited states (•••••) that contribute to the vibronic fine structures.

There are two main absorption peaks for the neutral oxidized FMN (around 380 nm and 450 nm). The calculated spectrum in the gas phase resembles the experimental one well, except for a blue-shift of the high-energy peak, while the inclusion of the PCM calculations effectively reduces this deviation. Similarly for the half-reduced semiquinone $FMNH^{\bullet}$ the spectrum calculated by including PCM matches the experimental data much better than that of the gas phase, exhibiting a main peak at 350 nm and a broad peak around 575 nm. However, for the reduced $FMNH^-$, an obvious difference between the spectra in the gas phase and the PCM environment can be found. In the former case, the calculated spectrum exhibits a strong absorption in the low-energy region (named as P1 hereafter) and a relative weak peak at the high-energy region (P2), while the situation is reversed in the PCM case. Figure 3 presents the selected molecular orbitals (MOs) involved in the main transitions leading to those two peaks. P1 in the gas phase is mainly due to a π-to-π^* transition (HOMO→HOMO+4) delocalized on the three aromatic rings, with an intensity (0.0442) much stronger than for P2 (0.0184), which has considerable electronic distribution to the Rydberg orbital. On the other hand, the two main peaks in the PCM calculations are all

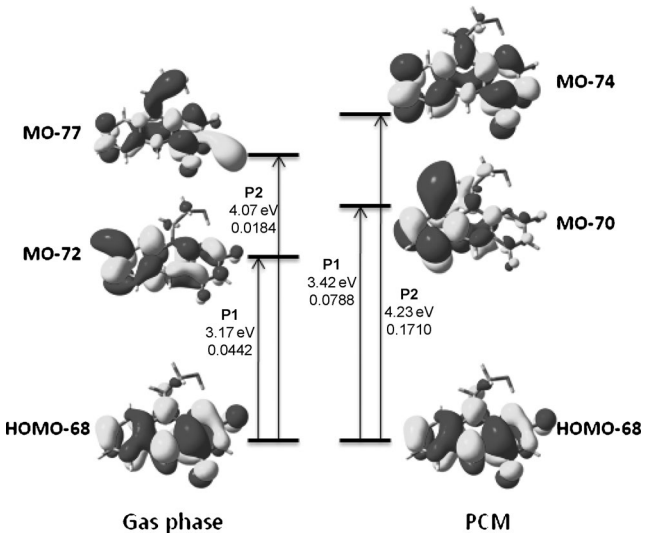

Figure 3. Selected MOs involved in excitations in the gas phase and including PCM for $FMNH^-$.

strong $^1\pi\pi^*$ transitions and P2 is twice as strong as P1. Therefore, we conclude that it is the different intrinsic electronic excitations that induce the changes in the spectra. The spectrum calculated by including PCM corresponds better to experiment. It should be noted that some discrepancy may originate from the limitation of LCM, which assumes the same potential energy surface curvatures between the ground state and the excited state.

From the discussions above, one can conclude that while the external implicit-solvent environment has little influence on the spectra of oxidized and half-reduced species, it does affect the spectra of fully reduced species. This influence arises mainly from the intrinsic structural change and charge redistribution during the redox cycle process. It is the innate character of FMN that initiates the adaptation of the surrounding implicit solvent and ultimately dictates its spectral characteristics. Our recent work on the other flavin molecule $FADH^-$[13] showed that the internal intramolecular hydrogen bonding likewise induces significant changes in the emission spectra.

The specific environment (such as hydrogen bonds and protein environment) is thought to have a strong influence on the spectra of flavins.[6b] From the oxidized FMN to the half-reduced $FMNH^\bullet$, N5 becomes protonated and forms a hydrogen bond to the carbonyl group of Glycine 61 (G61), as indicated by structural analysis.[6a] The stabilization by this external hydrogen bond is believed to account for the observed change in redox potential.[6a,b] Would it really be possible to reveal these important microscopic details from the optical spectra? To examine this, we enlarged our model by including the hydrogen bond of G61 to $FMNH^\bullet$ shown in Figure 4a. In the optimized geometric structure of $FMNH^\bullet$/G61, the hydrogen bond between the oxygen atom of glycine and N5 is 2.06 Å. As shown in Figure 4a, compared to the $FMNH^\bullet$ model, the calculated spectrum with the G61 (——) is almost identical to that without the G61 (-----). There is only a small blue-shift in the low-energy region. This implies that the external hydrogen

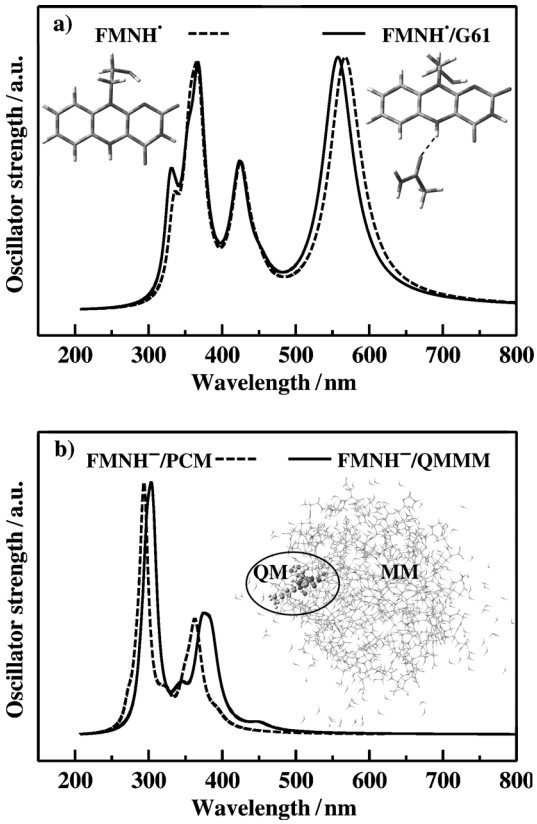

Figure 4. Calculated oscillator strengths. The inset in (b) shows the structure of the ONIOM model used for the calculation.

bond has little influence on the absorption spectrum of $FMNH^\bullet$.

Chang et al.proposed that from $FMNH^\bullet$ to fully reduced $FMNH^-$ the repulsion between $FMNH^-$ and the negatively charged surrounding residues induces local structure that is more flexible and solvated faster.[3] To explore the effects of protein structural constraints on the optical spectrum of the $FMNH^-$ we employed the ONIOM method[10] (B3LYP:Amber). Due to computational difficulties and in order to make direct comparisons, the model system in the QM part was extracted for the calculations of excitation energy and oscillator strength at TDDFT level. The calculated electronic absorption spectra by the ONIOM method are compared with the PCM results in Figure 4b. The good correspondence between these two calculated spectra indicates again that the underlying reason for such local structure flexibility arises mainly from the butterfly bending motion which is an intrinsic property of the molecule itself. It is worth to stress that although we cannot give the detailed dynamic picture of specific environmental structures from static spectral calculations, our present work confirms the importance of the intrinsic properties of FMN molecules on their optical spectra. It is quite interesting to see that the biomolecule can "feel" the change of the specific environment and respond to it by modifying its own internal properties.

To summarize, the calculated absorption spectra successfully clarified the spectral differences between the three redox states of FMN as the result of the changes in their intrinsic

properties and highlighted the self-regulation ability of those biomolecules. Our work stresses the decisive role of the internal property of FMN in the determination of the spectral characteristics and maybe even of other biological functions.

Acknowledgements

The work was supported by the Swedish National Infrastructure for Computing (SNIC), the Nature Science Foundation of China (20720102038, 20925311), and the Major State Basic Research Development Programs of China (2010CB923300).

Keywords: density functional calculations · flavin mononucleotides · flavodoxins · redox chemistry · vibrational resolved spectroscopy

[1] S. Sporlein, H. Carstens, H. Satzger, C. Renner, R. Behrendt, L. Moroder, P. Tavan, W. Zinth, J. Wachtveitl, *Proc. Natl. Acad. Sci. USA* **2002**, *99*, 7998 – 8002.
[2] H. Neuweiler, S. Doose, M. Sauer, *Proc. Natl. Acad. Sci. USA* **2005**, *102*, 16650 – 16655.
[3] C. W. Chang, T. F. He, L. J. Guo, J. A. Stevens, T. P. Li, L. J. Wang, D. P. Zhong, *J. Am. Chem. Soc.* **2010**, *132*, 12741 – 12747.
[4] H. Yang, G. B. Luo, P. Karnchanaphanurach, T. M. Louie, I. Rech, S. Cova, L. Y. Xun, X. S. Xie, *Science* **2003**, *302*, 262 – 266.
[5] M. Kondoh, K. Hitomi, J. Yamamoto, T. Todo, S. Iwai, E. D. Getzoff, M. Terazima, *J. Am. Chem. Soc.* **2011**, *133*, 2183 – 2191.
[6] a) R. P. Simondsen, G. Tollin, *Mol. Cell. Biochem.* **1980**, *33*, 13 – 24; b) J. Sancho, *Cell. Mol. Life Sci.* **2006**, *63*, 855 – 864; c) F. Müller, *Top. Curr. Chem.* **1983**, *108*, 71 – 107.
[7] W. Watt, A. Tulinsky, R. P. Swenson, K. D. Watenpaugh, *J. Mol. Biol.* **1991**, *218*, 195 – 208.
[8] a) J. Tomasi, B. Mennucci, R. Cammi, *Chem. Rev.* **2005**, *105*, 2999 – 3093; b) M. Cossi, G. Scalmani, N. Rega, V. Barone, *J. Chem. Phys.* **2002**, *117*, 43 – 54; c) M. Cossi, V. Barone, *J. Chem. Phys.* **2001**, *115*, 4708 – 4717.
[9] P. E. M. Siegbahn, M. R. A. Blomberg, *Chem. Rev.* **2010**, *110*, 7040 – 7061.
[10] S. Dapprich, I. Komaromi, K. S. Byun, K. Morokuma, M. J. Frisch, *Theochem-J. Mol. Struct.* **1999**, *461*, 1 – 21.
[11] Gaussian 09 (Revision B.01), M. J. Frisch, G. W. Trucks, H. B. Schlegel, G. E. Scuseria, M. A. Robb, J. R. Cheeseman, G. Scalmani, V. Barone, B. Mennucci, G. A. Petersson, H. Nakatsuji, M. Caricato, X. Li, H. P. Hratchian, A. F. Izmaylov, J. Bloino, G. Zheng, J. L. Sonnenberg, M. Hada, M. Ehara, K. Toyota, R. Fukuda, J. Hasegawa, M. Ishida, T. Nakajima, Y. Honda, O. Kitao, H. Nakai, T. Vreven, J. A. Montgomery, Jr., J. E. Peralta, F. Ogliaro, M. Bearpark, J. J. Heyd, E. Brothers, K. N. Kudin, V. N. Staroverov, R. Kobayashi, J. Normand, K. Raghavachari, A. Rendell, J. C. Burant, S. S. Iyengar, J. Tomasi, M. Cossi, N. Rega, J. M. Millam, M. Klene, J. E. Knox, J. B. Cross, V. Bakken, C. Adamo, J. Jaramillo, R. Gomperts, R. E. Stratmann, O. Yazyev, A. J. Austin, R. Cammi, C. Pomelli, J. W. Ochterski, R. L. Martin, K. Morokuma, V. G. Zakrzewski, G. A. Voth, P. Salvador, J. J. Dannenberg, S. Dapprich, A. D. Daniels, Ö. Farkas, J. B. Foresman, J. V. Ortiz, J. Cioslowski, and D. J. Fox, Gaussian, Inc., Wallingford CT, **2009**.
[12] a) P. Macak, Y. Luo, H. Agren, *Chem. Phys. Lett.* **2000**, *330*, 447 – 456; b) B. Minaev, Y. H. Wang, C. K. Wang, Y. Luo, H. Agren, *Spectroc. Acta Pt. A Molec. Biomolec. Spectr.* **2006**, *65*, 308 – 323.
[13] Y. J. Ai, F. Zhang, S. F. Chen, Y. Luo, W. H. Fang, *J. Phys. Chem. Lett.* **2010**, *1*, 743 – 747.
[14] Y. J. Zheng, R. L. Ornstein, *J. Am. Chem. Soc.* **1996**, *118*, 9402 – 9408.

Received: August 30, 2011
Published online on September 26, 2011

